SHOCK, Vol. 35, No. 5, pp. 506–511, 2011

SUPPRESSION OF AUTOPHAGY IN RAT LIVER AT LATE STAGE OF POLYMICROBIAL SEPSIS

Wei-Shan Chien,* Yen-Hsu Chen,†‡ Pei-Chi Chiang,* Hsiu-Wen Hsiao,* Shu-Mien Chuang,† Sheng-I Lue,* and Chin Hsu*

**Department of Physiology, Faculty of Medicine, †Graduate Institute of Medicine, College of Medicine, Kaohsiung Medical University; and ‡Department of Internal Medicine, Division of Infectious Diseases, Kaohsiung Medical University Hospital, Kaohsiung, Taiwan*

Received 21 Oct 2010; first review completed 9 Nov 2010; accepted in final form 6 Dec 2010

ABSTRACT—Sepsis develops as a result of the host response to infection, and its mortality rate in ICU remains high. Severe inflammation usually causes overproductions of proinflammatory cytokines, i.e., TNF-α and reactive oxygen species, which lead to mitochondrial damage and energetic depletion. Autophagy is a survival mechanism for eukaryote to recycle intracellular nutrients and maintain energy homeostasis. We hypothesize that autophagy plays a beneficial role in the pathogenesis of organ failure during sepsis. A rat model of cecal ligation and puncture (CLP) that simulate peritonitis-induced sepsis was used, and indicators for liver dysfunction, serum glutamic oxaloacetic, serum glutamic pyruvic, alkaline phosphatase, and bilirubin were measured. Levels of LC3-II and LC3 aggregation were quantified by Western blot analysis and by immunohistochemistry, respectively. The tissue localization of autophagy was identified by immunohistochemistry and transmission electron microscopy. Our results showed that (*a*) increase in LC3-II level in liver tissue occurs at 3 h, peaks at 6 h, and then surprisingly declines quickly until 18 h after CLP (CLP_{18h}); (*b*) significant hepatic dysfunction was observed at CLP_{18h}; (*c*) ratio of LC3 aggregation is significantly higher in hepatocytes than in Kupffer cells, and (*d*) loss of Atg7, an essential gene for autophagosome formation, exaggerates the TNF-α–induced cell death, depletion of ATP, and decrease of albumin production in hepatocytes. These results indicate that autophagy occurs transiently in hepatocytes at early stage, and the decline in autophagy at late stage may contribute to the functional failure in liver during polymicrobial sepsis.

KEYWORDS—Organ failure, CLP, macroautophagy

INTRODUCTION

Sepsis develops as a result of the host response to severe infection (1, 2). In recent years, a growing body of evidence suggests that liver failure develops during sepsis mainly as a consequence of mitochondrial dysfunction and cellular energy depletion (3). However, the role of endogenous survival response such as autophagy, which is an intracellular protein quality control system (4, 5) and is also an adaptive response to combat critical illness, has yet to be deciphered in detail at the *in vivo* level. It is essential to delineate the role of autophagy in response to septic insult for establishing therapeutic interventions for prevention of hepatic failure during sepsis.

Sepsis is characterized by systematic inflammation where secretion of proinflammatory cytokines (i.e., TNF-α) and subsequent overproduction of reactive oxygen species (ROS) lead to mitochondrial damage (6, 7). Treatment of MitoQ, an antioxidant selectively targeted at mitochondria, protects against organ damage after LPS treatment (8), implying the contribution of mitochondrial ROS overproduction to organ failure. Simultaneously, oxidative stress and mitochondrial injury trigger macroautophagy (9, 10), one of three types of mammalian autophagy (11). Macroautophagy (hereafter referred to as autophagy) sequesters whole organelles or portions of cytoplasm into autophagic vacuoles (autophagosomes) that fuse with lysosomes and undergo degradation. Autophagy in liver is important for the balance of energy and nutrients, removal of misfolded proteins, and turnover of major subcellular organelles (12). In general, autophagy promotes survival by removing unwanted cellular substances and by providing nutrients during starvation. It could, however, also contribute to cell death if the process is deregulated (12, 13). When cells need to rid themselves of damaged cytoplasmic components or to eliminate damaged organelles, autophagy is rapidly upregulated (14). However, little is known about the role of autophagy specifically in hepatic failure during sepsis.

Recent report showed that autophagic vacuolization increases and is associated with mitochondrial injury in the liver of septic patient (15). Furthermore, administration of LPS, a major component of bacterial outer walls, leads to liver injury associated with an increase in autophagy (16). Given that autophagy is a cellular response to stress, we propose that autophagy would play a beneficial role in hepatic failure during sepsis. Although what determines whether autophagy will be harmful or protective to the cell remains unknown, the level andduration of autophagy may play a critical role in maintaining organ functional homeostasis. Therefore, time-course changes of autophagy and hepatic function *in vivo* were observed to decipher whether sustained accumulation of autophagy results in hepatic failure, or a transient adaptive autophagy fails to protect the liver from septic damage. Loss of autophagic function attributed to siRNA of Atg7, an essential gene for autophagosome formation, was used to examine the role of autophagy in TNF-α–induced hepatocyte dysfunction. We found

Address reprint requests to Chin Hsu, PhD, Department of Physiology, Faculty of Medicine, College of Medicine, Kaohsiung Medical University, No. 100, Shih-Chuan 1st Rd, Kaohsiung 807, Taiwan. E-mail: chinhsu@kmu.edu.tw.

W.-S.C. and Y.-H.C. contributed equally to this work.

This study was supported by grants from the National Science Council, Taiwan (96-2320-B-037-028-MY3 and 96-2314-B-037-018-MY3).
DOI: 10.1097/SHK.0b013e31820b2f05
Copyright © 2011 by the Shock Society

Copyright © 2011 by the Shock Society. Unauthorized reproduction of this article is prohibited.

that loss of autophagy exaggerates TNF-α–induced dysfunction in hepatocytes.

MATERIALS AND METHODS

Animal model

Male Sprague-Dawley rats weighing 250 to 350 g were purchased from the National Experimental Animal Center (Nan-Kang, Taipei, Taiwan) and were bred in Kaohsiung Medical University animal center with light-dark cycle of 12:12 h. Rats were divided randomly into sham-operated and cecal ligation and puncture (CLP) groups. All the rats were fasted overnight but with free access to water before CLP operation. Under anesthesia, CLP was performed according to the method of Wichterman et al. (17). In brief, a laparotomy was performed, and the cecum was ligated with a 3-0 silk ligature and punctured in two sites with an 18-gauge needle. The cecum was then returned to the peritoneal cavity, and the abdomen was closed in two layers. Control rats were sham-operated (a laparotomy was performed, and the cecum was manipulated but neither ligated nor punctured). The liver tissues were sampled at 3, 6, 9, and 18 h after CLP for further immunoblot and immunohistochemistry analyses. All the animal experiments were performed according to the guidelines of the National Institutes of Health and were approved by the Kaohsiung Medical University Committee for the Use of Experimental Animals.

Western blotting

Liver tissues were sampled, homogenized in 400 μL lysis buffer (50 mM Tris acetate [pH 7.4]; 5 mM EDTA) and then centrifuged at 14,000 revolutions per minute for 30 min. Protein concentration of the supernatant was determined by protein assay kit (Bio-Rad Corp, Hercules, Calif). For LC3-II detection, equal amounts (40 μg) of protein from each sample were separated by 15% sodium dodecyl sulfate (SDS)–polyacrylamide gel electrophoresis and transferred onto a polyvinylidene difluoride membrane (NEN Life Science Products, Boston, Mass). The membranes were incubated with t-TBS containing 5% nonfat milk before incubation with primary rabbit anti-LC3B antibody (Sigma, St. Louis, Mo) at 1,000× dilution followed by secondary goat anti–rabbit IgG (Santa Cruz, San Francisco, Calif) at 1,000× dilution to recognize the primary antibody. For the detection of Atg7, equal amounts (20 μg) of protein from each sample were separated by 9% SDS gel electrophoresis and transferred to polyvinylidene difluoride membrane. The membranes were incubated with primary mouse anti Atg7 antibody (Biosensis, Thebarton, South Australia) at 1,000× dilution. Then, secondary goat anti–rabbit IgG (Santa Cruz) at 5,000× dilution was utilized to recognize the primary antibody. β-Actin was used as a sample loading control. After incubation, the membranes were developed by enhanced chemiluminescence (PerkinElmer Life and Analytical Science, Boston, Mass) and subsequently exposed to x-ray film (Fuji, Tokyo, Japan).

Immunohistochemistry

Rats were anesthetized with pentobarbital (35 mg/kg body weight, i.p.) and perfusion with 0.9% normal saline through the left ventricle. Rat liver was removed immediately and fixed by 4% paraformaldehyde for 24 h, then immersed in 30% sucrose solution for 24 h, and embedded in frozen tissue matrix (optimal cutting temperature; Sakura Finetek USA, Inc, Torrance, Calif). Optimal cutting temperature–embedded tissues were sectioned in 5-μm thickness. The frozen sections were briefly rinsed in 0.1 M phosphate-buffered saline (PBS) and subsequently incubated with 3% H_2O_2 solution in methanol for 15 min to quench endogenous peroxidase activity. Subsequently, these sections were incubated with blocking solution containing 1% bovine serum albumin (Sigma Chemical Co, St. Louis, Mo), 10% normal goat serum (Jackson ImmunoResearch Laboratories, Inc, West Grove, Pa) and 1% Triton X-100 for 1 h at room temperature. Then, sections were incubated with anti-LC3B antibody (Sigma-Aldrich, St. Louis, Mo) 1:50 dilution at room temperature for 2 h followed by incubation at 4°C overnight. After having been washed three times with 0.1 M PBS containing 0.5% Triton X-100 for 10 min each time, the sections were incubated with fluorescein isothiocyanate (FITC)–conjugated AffiniPure goat anti–rabbit IgG 1:500 dilution (Jackson ImmunoResearch Laboratories, Inc) or with rhodamine-conjugated AffiniPure goat anti–rabbit IgG (Jackson ImmunoResearch Laboratories, Inc) for 1 h at room temperature. Then, sections were mounted with fluorescent mounting medium (Dako Cytomation, Carpinteria, Calif) after washing. Images were acquired using a fluorescence microscope (Zeiss AxioVert 200M; Carl Zeiss MicroImaging GmbH, Jena, Germany) equipped with a computer-controlled mechanical stage and a CoolSNAP EZ Camera (Roper Scientific GmbH Germany, Munich, Germany). Image acquisition was controlled by RSImage (Photometrics, Tucson, Ariz) and Image J (National Institutes of Health) software.

Biochemical measurements of liver functions

Blood samples were collected from tail vein at 6, 9, and 18 h after CLP. The serum levels of serum glutamic oxaloacetic (SGOT), serum glutamic pyruvic (SGPT), alkaline phosphatase (ALP), total bilirubin (TBIL), and direct bilirubin (DBIL) were measured to monitor the hepatic function. Levels of SGOT and SGPT were estimated by a colorimetric kit, following the manufacturer's protocol. Briefly, a 20-μL serum was added to the reaction solution. The resultant reaction mixture was incubated at 37°C for 30 min (SGPT) or 60 min (SGOT), and the absorbance of the solution was determined at 505 nm using a microplate reader. Total bilirubin or DBIL concentration was measured by an end-point diazo method. In the reaction, the bilirubin reacts with diazo reagent in the presence of caffeine, benzoate, and acetate as accelerators to form azobilirubin. Direct bilirubin concentration was also estimated by an end-point diazo method. In the reaction, DBIL combines with diazo to form azobilirubin. The system monitors the change in absorbance at 520 nm. The change in absorbance is directly proportional to the concentration of bilirubin in the sample. The concentrations of TBIL, DBIL, and ALP were determined by Beckman Synchron LX20 System (Beckman-Coulter, Fullerton, Calif).

Transmission electron microscopy

Liver tissues were sampled from rats at 6 h after CLP, dissected into 1-mm^3 pieces, and then immersed in a fresh 2% paraformaldehyde plus 2.5% glutaraldehyde in 0.1 M PBS overnight. Then, the tissues were fixed with 2% osmium tetroxide at 4°C for 90 min and dehydrated by graded percentage of alcohol (50%, 75%, 85%, 95%, and 100%). The tissue block was then embedded in Epon (Sigma-Aldrich, St. Louis, Mo). Ultrathin sections (70 nm) were prepared with an automatic ultramicrotome (Reichert Ultracut E, Vienna, Austria) using a diamond knife and then stained with uranyl acetate and lead citrate solutions. Sections were collected on nickel grids (200 mesh) and examined by transmission electron microscope (JEM2000 EXII; Jeol Ltd, Tokyo, Japan).

Isolation of Kupffer cells and hepatocytes

To isolate Kupffer cells and hepatocytes, rats were anaesthetized and killed at 6 h after sham operation or CLP. Kupffer cells and hepatocytes were isolated as described elsewhere (18), with slight modification. Briefly, the portal vein was cannulated following a midline incision, and the inferior vena cava was severed. The liver was immediately perfused *in situ* with approximately 120 to 150 mL of Hanks balanced salt solution (HBSS; contained 0.05% EDTA, without calcium and magnesium, at 37°C, and continuously gassed with O_2/CO_2 [19:1]) at a rate of approximately 10 to 12 mL/min. This was followed by perfusion of approximately 100 mL of HBSS containing 0.05% collagenase type IV (#C0130 or #Ct183, 100 U/mL; Sigma) at 37°C. The liver tissue was minced in a Petri dish containing HBSS and centrifuged (600 revolutions per minute, 10 min, at 4°C); above procedure was repeated three times to sediment hepatocytes. The cell pellets were then resuspended (5×10^5/mL) in HBSS and further purified with 50% Percoll (Sigma-Aldrich). Cell viability was greater than 90% as determined by trypan blue exclusion test. The non–parenchymal cell–enriched supernatant was centrifuged at 800*g* for 10 min; the pellet was resuspended in 40 mL of PBS. The supernatant enriched with Kupffer cells was diluted in PBS and centrifuged at 800*g* for 10 min. The resulting pellet was resuspended in culture medium (RPMI 1640 with 10% fetal calf serum) at a concentration of 1.0×10^6 cells/mL. Kupffer cells were selected by allowing them to adhere for 2 h at 37°C in an atmosphere with 50 mL/L CO_2. After removing nonadherent cells by gentle washing, adherent cells were incubated in RPMI 1640. More than 95% of adherent cells were esterase-positive.

After isolation, the cells were fixed by 4% paraformaldehyde for 5 min and were attached on the slide by using cytospin at 1,500 revolutions per minute for 5 min. Before immunostaining, the cells were air dried for 2 h, rinsed by 0.1 M PBS, and then incubated with 0.3% H_2O_2 in methanol for 15 min to quench the endogenous autofluorescence and incubated with 10% normal gout serum (mixed with 1% bovine serum albumin and 1% Triton X-100) at room temperature for 30 min to block the nonspecific binding. Then, the cells were incubated with LC3B antibody at 4°C (1:100) overnight, followed by incubation with second antibody (goat anti–rabbit FITC; Jackson ImmunoResearch Laboratories, Inc) at room temperature for another 1 h. The images of immunocytochemistry were acquired on an OlymPus IX71 confocal laser scanning system (Olympus Corp., Tokyo, Japan) using a 100× immersion objective or were examined under the 63× oil-immersion objective lens of a Zeiss AxioVert 200M fluorescence microscope (Carl Zeiss MicroImaging GmbH).

Transfection of Atg7 siRNA

Before transfection, 2×10^6 rat hepatocytes were seeded in a 6-cm dish for 24 h and then transfected with 100 nM Atg7 siRNA using transfection reagent (Dharmacon, Lafayette, Colo). The Atg7-targeting sense sequence

Copyright © 2011 by the Shock Society. Unauthorized reproduction of this article is prohibited.

contains four duplexes: 3′CAAAGUUAACAGUCGGUGUUU5′, 5′PACACC GACUGUUAACUUUGUU3′; 3′AGUGAAUGCCAGCGGGUUCUU5′, 5′PG AACCCGUGGCAUUCACUUU3′; 3′GUGGAGGAACUCAUCGAUAUU5′, 5′PUAUCGAUGAGUUCCUCCAGUU3′; and 3′CCCAGAAGAAGUUGAA GGAUU5′, 5′PUCGUUCAACUUCUUCUGGGUU3′ (NM_001012097), which were synthesized by Dharmacon. Nontargeted siRNA provided by Dharmacon was used as a negative control. Six hours after siRNA treatment, the medium containing transfection reagent was replaced with complete medium and recovered for 48 h. Then, the hepatocytes were harvested and lysed by adding lysis buffer (150 mM NaCl, 50 mM Tris-base [pH 7.5], 5 mM EDTA, 50 mM NaF, 0.1 mM sodium orthovanadate, 1% Triton X-100, and complete protease inhibitor mixture [Roche Applied Science, Indianapolis, Ind]). The protein levels of Atg7 and LC3-II were examined by Western blot analysis using 9% and 15% SDS–polyacrylamide gel electrophoresis, respectively, to confirm the knockdown efficiency of Atg7 siRNA.

Treatment of TNF-α

Hepatocytes at a concentration of 2×10^6 cells/mL were pretreated with 400 nM Act-D (Boehringer Mannheim, Mannheim, Germany) for 30 min in F-12K medium containing 2.5% fetal bovine serum. Then, they were incubated with 2 ng/mL recombinant TNF-α (Biosource, San Francisco, Calif) for 14 h to assess the effect of TNF-α exposure on ATP content, albumin production, and survival rate of hepatocytes (19).

Assay of ATP content

The ATP content in hepatocytes was measured using the ATPlite luminescence ATP detection assay system (PerkinElmer Life and Analytical Science) according to the manufacturer's instructions. In brief, hepatocytes were seeded in a 96-well culture plate at 2×10^3 cells/100 μL. After TNF-α treatment for 14 h, 50-μL cell lysis solution (Sigma) was added and shaken for 5 min to lyse the hepatocytes. Then, 50 μL of substrate (luciferase/lucerin) was added and shaken for another 5 min. The luminescence was then detected by plate chameleon (Chidex Ltd, Turku, Finland), and the ATP content in hepatocytes was estimated according to the standard curve.

Measurement of albumin production from hepatocytes

We used the AssayMax rat albumin enzyme-linked immunosorbent assay kit (AssayPro, Charles, Mo) to measure the level of albumin in the medium of cultured hepatocytes. In brief, 50-μL standard or sample was added into the well of the enzyme-linked immunosorbent assay kit. The wells were covered with a sealing tape, incubated for 1 h at room temperature, and washed five times with 200-μL wash buffer. Then, 50 μL of biotinylated rat albumin antibody was added to each well, incubated for 30 min, and washed five times with 200-μL wash buffer. Again, 50 μL of streptavidin-peroxidase conjugate was added to each well, incubated for 30 min, and washed five times with 200-μL wash buffer. Finally, 50 μL of chromogen substrate was added per well and incubated for 7 min, and 50-μL stop solution was added to each well. After all of the steps, the absorbance was immediately read on a microplate reader at a wavelength of 450 nm. Then, the optical density value was measured, and the concentration of albumin was extrapolated from standard curve.

Cell viability

Hepatocytes were trypsinized at 14 h after TNF-α treatment by incubation with trypsin-EDTA (Gibco, Langley, Okla) at 37°C for 5 min. Viability of the cells was determined by trypan blue exclusion test using hemocytometer.

Statistics

Data of experimental and control groups were evaluated statistically by one-way ANOVA followed by Scheffé post hoc test. Difference at $P < 0.05$ is considered significant.

RESULTS

Early transient elevation followed by suppression of autophagy in the rat liver after CLP

To understand the time-course change of autophagy in liver, a high-energy–demanding organ, during sepsis, we used the rat model of CLP that simulates human peritonitis-induced sepsis to study the possible role of autophagy in sepsis. The liver tissue was sampled at 3, 6, 9, and 18 h after CLP. An autophagosome-specific marker, conversion of LC3-I to LC3-II, was quantified by Western blot analysis, and the amount of LC3 aggregation was quantified under fluorescence microscope after immunohistochemical staining. The results showed that the basal level of LC3-II was low, and after CLP, the LC3-II protein level was transiently increased at 3 h ($P < 0.05$), peaked at 6 h ($P < 0.05$), but declined from 9 h until 18 h (Fig. 1A). The quantitative results of LC3-II aggregation in liver sections (Fig. 1B) showed similar trends as the immunoblot in the homogenate of liver tissue. In the sham group, most of the LC3-positive green color was distributed in the cytosol in a smeared manner, which indicates uncleaved LC3-I pervades in cytosol, as shown in the upper panel of Figure 1B. In CLP groups, the number of the bright green dots, which indicates LC3 lipidation/aggregation in autophagosomes, as the arrow indicated, was significantly increased at 6 h after CLP ($P < 0.01$), whereas the number of LC3 aggregation dots was significantly decreased at 9 and 18 h after CLP.

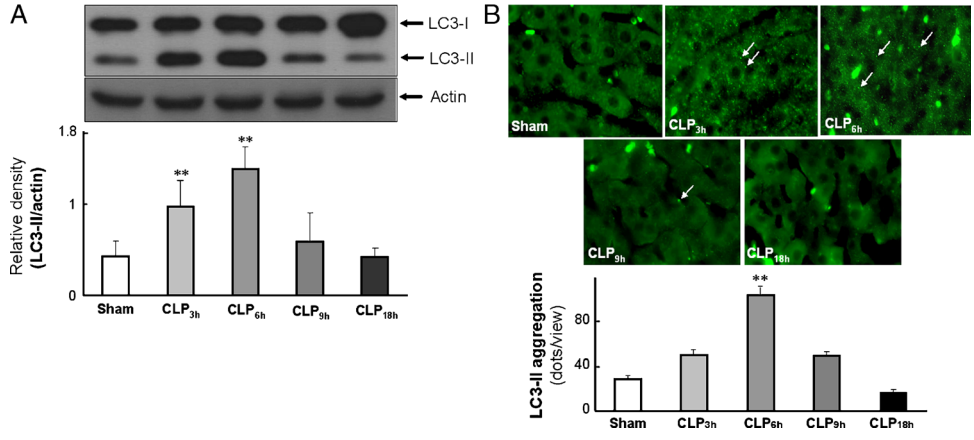

FIG. 1. **A transient increase followed by suppression of autophagy in rat liver during sepsis**. A, Time-course change of LC3-II in liver tissue. Cecal ligation and puncture were performed to simulate peritonitis and subsequent sepsis. Liver tissue was sampled at 3, 6, 9, and 18 h after CLP (CLP_{3h}, CLP_{6h}, CLP_{9h}, CLP_{18h}). The protein abundance of LC3-II was quantified by Western blot analysis. β-Actin was used as a loading control. The molecular weights of LC3-I, LC3-II, and β-actin are 16, 18, and 43 kd, respectively. A representative Western blot is shown in the upper panel of the lower quantitative result. B, LC3 aggregation in liver tissue. Liver tissue was fixed after perfusion. Tissue was sectioned in 5-μm thickness, and LC3 aggregation was quantified under fluorescence microscope after immunostaining with LC3B antibody followed by second antibody conjugated with FITC. LC3 aggregation was estimated by counting the number of bright green dots, as arrows indicated under the field of microscope with 200× amplifications. Ten fields were randomly selected for counting per section. Three liver sections were chosen per rat. A representative image is shown in the upper panel of the lower quantitative result. Quantitative data show mean ± SD of eight liver samples from eight different rats, $*P < 0.05$, $**P < 0.01$.

Copyright © 2011 by the Shock Society. Unauthorized reproduction of this article is prohibited.

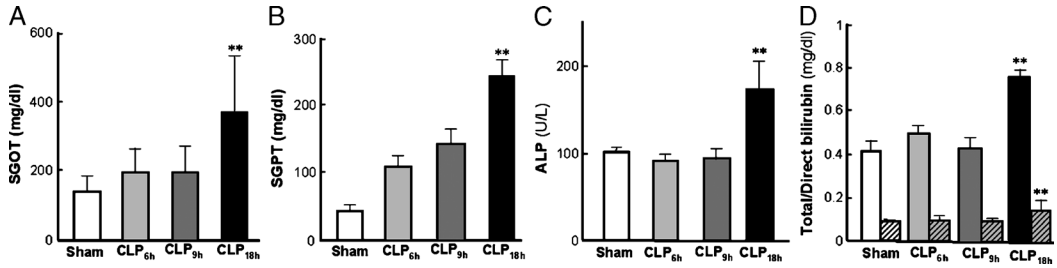

FIG. 2. **Hepatic dysfunction occurred at the late stage of sepsis**. A, SGOT. B, SGPT. C, ALP. D, TBIL (blank column) and DBIL (hatch column). Cecal ligation and puncture were performed to induce peritonitis and subsequent sepsis. Serum was sampled at 6, 9, and 18 h after CLP. Data are shown as mean ± SD of 6 rats. $^{**}P < 0.01$.

Hepatic dysfunction occurred at late stage of sepsis

To study the time-course relationship between autophagy and liver dysfunction, we checked the indexes of liver dysfunction at 6, 9, and 18 h after CLP. The result showed significant elevations of SGOT (Fig. 2A), SGPT (Fig. 2B), ALP (Fig. 2C), and both TBILand DBIL (Fig. 2D) at 18 h after CLP.

Autophagy occurred primarily in hepatocytes during sepsis

To delineate the major cell type in liver tissue where autophagy occurred during sepsis, we examined the liver tissue at 6 h after CLP by confocal microscope and electron microscope. As Figure 3A shows, the large-size nuclei stained by DAPI (blue color), as the arrowhead indicated, are hepatocytes. Only few green LC3 aggregation dots were observed in liver tissue of the sham group, whereas more LC3 aggregation dots around the nucleus of hepatocyte were observed in liver tissue of CLP_{6h} group. The hepatic ultrastructure showed intact mitochondria in the hepatocyte of the sham-operated group, as shown in the left panel of Figure 3B, whereas some swelling mitochondria engulfed by double-membrane autophagosome were observed in the hepatocytes of the CLP_{6h} group, as shown in the second picture in Figure 3B. In Kupffer cells, the whole cell was almost occupied by the nucleus, as shown in the third picture of Figure 3B. Fewer mitochondria were found, and no autophagosome-like structure was observed in Kupffer cells, as shown in the fourth picture of Figure 3B.

For further quantification of autophagy, we isolated both hepatocytes and Kupffer cells from the liver of septic rat at CLP_{6h} and quantified the percentage of LC3 aggregation–positive cells after immunofluorescence staining using LC3B antibody. The results showed that, in hepatocytes, the autophagic incidence of the CLP_{6h} group (61%) was significantly higher than that of sham group (28%) ($P < 0.01$). In Kupffer cells, only 6% of LC3-II aggregation–positive cells occurred in the sham group, and the autophagic incidence was increased by 6% ($P < 0.05$) in CLP_{6h} group.

Loss of autophagy exaggerates TNF-α–induced dysfunction in hepatocytes

To elucidate whether the decline in autophagy plays a harmful role in the late stage of sepsis, Atg7 siRNA was used to suppress autophagosome formation. Nontargeted siRNA

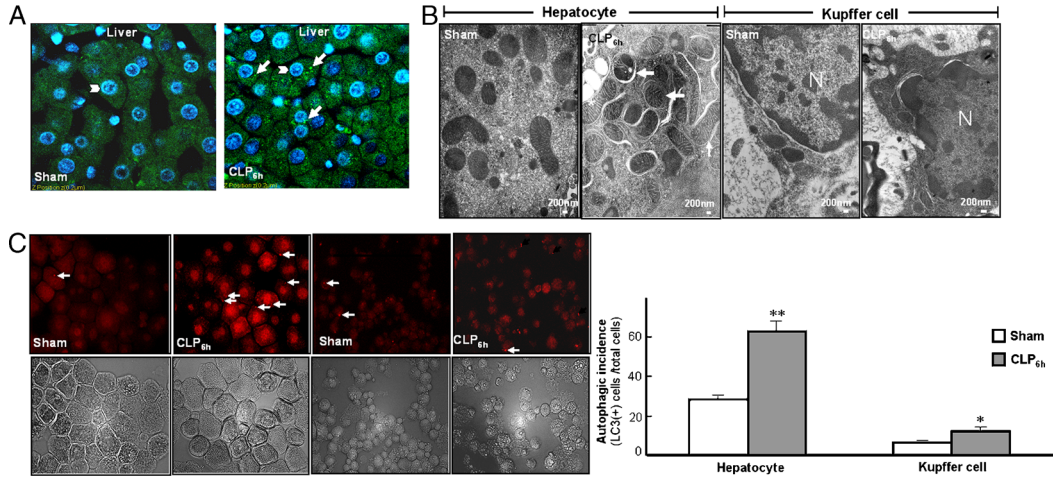

FIG. 3. **High level of the autophagy was observed in hepatocytes after CLP**. A, LC3-II aggregation in the septic liver. The liver tissue was sampled at 6 h after CLP (CLP_{6h}). Nuclear DNA was stained by DAPI. LC3-II aggregation was identified as a marker for autophagy under confocal microscope after staining with LC3B antibody followed by second antibody conjugated with FITC. The large-size nuclei stained by DAPI (blue color) indicated by arrowhead are hepatocytes. Bright green spots around the nucleus indicated by arrows represent LC3 aggregation (magnification ×600). B, The ultrastructure of septic liver. Ultrastructure was examined under transmission electron microscope. The left and right panels show the ultrastructures of hepatocyte and Kupffer cell, respectively. Arrows indicate the damaged or swelling mitochrondria, which were engulfed by double-membrane phagophore, in hepatocytes (magnification ×20,000). C, Autophagic ratio in hepatocytes or Kupffer cells derived from septic rats. Both hepatocytes and Kupffer cells were isolated from the liver of septic rat at 6 h after CLP (CLP_{6h}) and were adhered on a cover slip by cytospin and then stained by LC3B antibody followed by second antibody conjugated with rhodamine (red color shown in the upper panel). The bright-field images in the second row of the upper panel show the morphology of hepatocytes (left two images) or Kupffer cells (right two images) under phase contrast microscope. The cell contains more than three red spots counted as autophagy-positive cell. The autophagic ratio was expressed as the number of autophagy-positive cells divided by total number of cells. Ten fields per sample were randomly selected for counting. The quantitative data shown in the lower panel are expressed as mean ± SD of seven samples, $^{*}P < 0.05$, $^{**}P < 0.01$ (magnification ×400).

Copyright © 2011 by the Shock Society. Unauthorized reproduction of this article is prohibited.

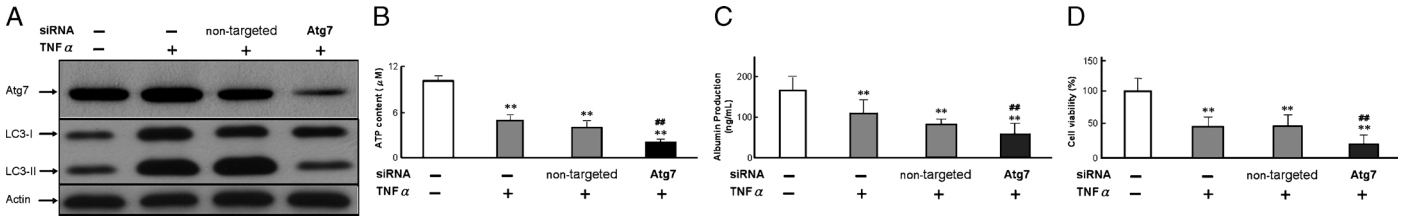

FIG. 4. **Knockdown Atg7 exaggerates TNF-α–induced dysfunction in hepatocytes**. A, Protein levels of Atg7 and LC3-II; (B) ATP content; (C) albumin production; (D) cell viability. Hepatocytes were isolated from liver of normal SD rat. Atg7 siRNA was added 36 h before exposure to TNF-α at a concentration of 2 ng/mL. After 14 h, culture medium was sampled for assay of albumin. Hepatocytes were harvested for assays of ATP content, cell viability, and Western blot analysis of Atg7, LC3-I, and LC3-II. The molecular weights of Atg7, LC3-I, LC3-II, and β-actin are 75, 18, 16, and 43 kd, respectively. Data shown in B, C, and D are mean ± SD of eight samples. $^{**}P < 0.01$ comparable to control group; $^{\#\#}P < 0.01$ comparable to nontargeted siRNA group.

was used as a negative control. Exposure to TNF-α simulates the *in vivo* proinflammatory cytokine milieu during sepsis. Three functional indexes (ATP content, albumin production, and cell survival rate) of hepatocytes were compared between Atg7 knockdown group and nontargeted siRNA group. The results showed that TNF-α exposure significantly decreases ATP content and albumin production as well as the survival rate of hepatocytes. Loss of autophagy by knockdown Atg7 using siRNA significantly exaggerates the TNF-α–induced dysfunction of hepatocytes, as shown in Figure 4.

DISCUSSION

This study aims to examine the role of autophagy in hepatic failure due to polymicrobial sepsis induced by CLP that simulates human peritonitis. In response to septic insult, a transient increase in the level of autophagy in liver, particularly hepatocytes, was observed. However, this transient increase of autophagy declined at CLP_{9h} until the late stage (CLP_{18h}) of sepsis, which was associated with hepatic failure. Specific knockdown of Atg7 exaggerates the TNF-α–induced hepatocyte dysfunction, implying a protective role of autophagy in proinflammatory cytokine-induced liver dysfunction during sepsis. Our findings suggest that the decline in the recycle function of autophagy at late stage may contribute to hepatic failure during sepsis.

Development of organ dysfunction during sepsis is due at least in part to excessive secretion TNF-α and oxidative damage to mitochondria (8, 20–22). Autophagy is an intracellular survival mechanism that is rapidly upregulated during cellular stress, such as oxidative stress or mitochondrial damage. In liver, autophagy is important for the balance of energy and nutrients for cell functions, the removal of misfolded proteins, the resistance to oxidative stress (23), and the turnover of mitochondria under both normal and pathophysiological conditions (12). In general, autophagy-mediated elimination of damaged organelles preserves cells from further damage (24). Previous report also indicated that hepatocyte resistance to injury from oxidative stress is mediated by function of autophagy, and impaired function of autophagy may promote oxidant-induced liver injury via overactivation of JNK signaling pathway that induces cell death (23). Consequently, the activation of autophagy is crucial to adaptation and survival under extreme conditions. Livers from patients who died of sepsis had significant increases in autophagic vacuolization compared with patients with elective liver biopsies (15). The findings in the livers of mouse model of sepsis (15) were similar to those of the clinical samples; however, a single time point level of autophagy was difficult to understand the role of autophagy during the progression of sepsis. In the present study, the time-course change of the levels of autophagy during the progression of sepsis in a rat model of CLP was examined. We found that the increase of the conversion of LC3-I to LC3-II in liver tissue occurs at 3 h, peaks at 6 h, and then declines from 9 h until 18 h after CLP. Accordingly, the initial elevation of autophagy may reflect the early host response to oxidative stress and mitochondrial damage caused by septic insult and may play a beneficial role in early stages of sepsis.

The challenge of elucidating the significance of autophagic response during sepsis is to determine whether autophagy prevents or contributes to organ failure at different stages of sepsis. There is an extensive number of studies reporting a harmful role for autophagy in type II programmed cell death or autophagic cell death (13) in human disease. Recent reports show that autophagy can act as both protector and killer of the cell, depending on the stage of the disease, the surrounding cellular environment, or the therapeutic interventions attempted (25). TNF-α–induced oxidative stress has been implicated as a central mechanism of a variety of forms of hepatic injury. Recent report indicated that mitochondrial damage due to TNF-α/ROS elicits late mitochondrial autophagy (26), and the overall process of autophagy is strongly ATP-dependent (27). Therefore, ROS, mitochondrial damage, and subsequent ATP depletion due to TNF-α exposure play critical roles in accelerating autophagy. Therefore, we use TNF-α to simulate the *in vivo* cytokine milieu during sepsis. The result showed that loss of autophagy exaggerates the hepatocytes dysfunction caused by exposure to TNF-α that simulates the *in vivo* proinflammatory cytokine milieu during sepsis (28). It implies that the decline in autophagy at late sepsis may cause insufficient recycle function, which contributes to hepatic failure. However, the reason why autophagy declines to basal level from CLP_{9h} until CLP_{18h} remains obscure.

Autophagy is a highly regulated process. According to the previous report, the septic insult triggers a rapid activation of transcription factor nuclear factor κB (NF-κB), with a peak occurring 3 h after CLP (29), and Djavaheri-Mergny et al. (30) indicated that NF-κB activation represses TNF-α–induced autophagy. In addition, it has been reported that insulin is a suppressor of autophagy (12, 31). During sepsis, hyperinsulinemia

Copyright © 2011 by the Shock Society. Unauthorized reproduction of this article is prohibited.

(32) and insulin resistance (33) were observed in the initial 5 h of rat model of CLP sepsis. The continuous increase in plasma insulin level can presumably inhibit autophagy and will evidently lead to retention of misfolded molecules and cellular dysfunction. Moreover, our previous report showed a bioenergetic failure occurred in the liver during late stage of sepsis (3). The results of the present study showed that elevation of LC3-II in septic liver occurred at 3 h, peaked at 6 h, and then declined until 18 h. Because the overall process of autophagy is strongly ATP-dependent (27), early activation of NF-κB and hyperinsulinemia, as well as late bioenergetic failure, may contribute to the suppression of autophagy at late sepsis. However, future studies can explore such possibilities to fully understand how autophagy is suppressed when it is highly needed for providing more recycle function to maintain intracellular energy homeostasis during sepsis.

In conclusion, pathophysiological conditions associated with an impairment of hepatic autophagic function may exaggerate liver dysfunction under oxidative stress due to severe inflammation. Our studies here provide some insights for understanding an important protective role for autophagy in rat model of CLP-induced sepsis. Further elucidation of the underlying mechanism of the suppression of autophagy at late stage of sepsis would shed light on a new approach for combating sepsis-induced hepatic failure.

REFERENCES

1. Gullo A, Bianco N, Berlot G: Management of severe sepsis and septic shock: challenges and recommendations. *Crit Care Clin* 22(3):489–501, 2006.
2. Vincent JL, Taccone F, Schmit X: Classification, incidence, and outcomes of sepsis and multiple organ failure. *Contrib Nephrol* 156:64–74, 2007.
3. Huang LJ, Hsu C, Tsai TN, Wang SJ, Yang RC: Suppression of mitochondrial ATPase inhibitor protein (IF1) in the liver of late septic rats. *Biochim Biophys Acta* 1767(7):888–896, 2007.
4. Heymann D: Autophagy: a protective mechanism in response to stress and inflammation. *Curr Opin Investig Drugs* 7(5):443–450, 2006.
5. Meijer AJ, Codogno P: Signalling and autophagy regulation in health, aging and disease. *Mol Aspects Med* 27(5–6):411–425, 2006.
6. Taylor DE, Ghio AJ, Piantadosi CA: Reactive oxygen species produced by liver mitochondria of rats in sepsis. *Arch Biochem Biophys* 316(1):70–76, 1995.
7. Zapelini PH, Rezin GT, Cardoso MR, Ritter C, Klamt F, Moreira JC, Streck EL, Dal-Pizzol F: Antioxidant treatment reverses mitochondrial dysfunction in a sepsis animal model. *Mitochondrion* 8(3):211–218, 2008.
8. Lowes DA, Thottakam BM, Webster NR, Murphy MP, Galley HF: The mitochondria-targeted antioxidant MitoQ protects against organ damage in a lipopolysaccharide-peptidoglycan model of sepsis. *Free Radic Biol Med* 45(11): 1559–1565, 2008.
9. Mijaljica D, Prescott M, Devenish RJ: Different fates of mitochondria: alternative ways for degradation? *Autophagy* 3(1):4–9, 2007.
10. Priault M, Salin B, Schaeffer J, Vallette FM, di Rago JP, Martinou JC: Impairing the bioenergetic status and the biogenesis of mitochondria triggers mitophagy in yeast. *Cell Death Differ* 12(12): 1613–1621, 2005.
11. Cuervo AM: Autophagy: many paths to the same end. *Mol Cell Biochem* 263(1–2):55–72, 2004.
12. Yin XM, Ding WX, Gao W: Autophagy in the liver. *Hepatology* 47(5): 1773–1785, 2008.
13. Bursch W, Ellinger A, Gerner C, Frohwein U, Schulte-Hermann R: Programmed cell death (PCD). Apoptosis, autophagic PCD, or others? *Ann N Y Acad Sci* 926:1–12, 2000.
14. Gustafsson AB, Gottlieb RA: Autophagy in ischemic heart disease. *Circ Res* 104(2):150–158, 2009.
15. Watanabe E, Muenzer JT, Hawkins WG, Davis CG, Dixon DJ, McDunn JE, Brackett DJ, Lerner MR, Swanson PE, Hotchkiss RS: Sepsis induces extensive autophagic vacuolization in hepatocytes: a clinical and laboratory-based study. *Lab Invest* 89(5):549–561, 2009.
16. Wang K, Damjanov I, Wan YJ: The protective role of pregnane X receptor in lipopolysaccharide/D-galactosamine–induced acute liver injury. *Lab Invest* 90(2):257–265, 2010.
17. Wichterman KA, Baue AE, Chaudry IH: Sepsis and septic shock—a review of laboratory models and a proposal. *J Surg Res* 29(2):189–201, 1980.
18. Smedsrod B, Johansson S, Pertoft H: Studies *in vivo* and *in vitro* on the uptake and degradation of soluble collagen alpha 1(I) chains in rat liver endothelial and Kupffer cells. *Biochem J* 228(2):415–424, 1985.
19. Yang RC, Jao HC, Huang LJ, Wang SJ, Hsu C: The essential role of PKCalpha in the protective effect of heat-shock pretreatment on TNFalpha-induced apoptosis in hepatic epithelial cell line. *Exp Cell Res* 296(2): 276–284, 2004.
20. Abraham E, Singer M: Mechanisms of sepsis-induced organ dysfunction. *Crit Care Med* 35(10):2408–2416, 2007.
21. Brealey D, Karyampudi S, Jacques TS, Novelli M, Stidwill R, Taylor V, Smolenski RT, Singer M: Mitochondrial dysfunction in a long-term rodent model of sepsis and organ failure. *Am J Physiol Regul Integr Comp Physiol* 286(3):R491–R497, 2004.
22. Vanhorebeek I, De Vos R, Mesotten D, Wouters PJ, De Wolf-Peeters C, Van den Berghe G: Protection of hepatocyte mitochondrial ultrastructure and function by strict blood glucose control with insulin in critically ill patients. *Lancet* 365(9453):53–59, 2005.
23. Wang Y, Singh R, Xiang Y, Czaja MJ: Macroautophagy and chaperone-mediated autophagy are required for hepatocyte resistance to oxidant stress. *Hepatology* 52(1):266–277, 2010.
24. Lemasters JJ, Qian T, He L, Kim JS, Elmore SP, Cascio WE, Brenner DA: Role of mitochondrial inner membrane permeabilization in necrotic cell death, apoptosis, and autophagy. *Antioxid Redox Signal* 4(5):769–781, 2002.
25. Ogier-Denis E, Codogno P: Autophagy: a barrier or an adaptive response to cancer. *Biochim Biophys Acta* 1603(2):113–128, 2003.
26. Baregamian N, Song J, Bailey CE, Papaconstantinou J, Evers BM, Chung DH: Tumor necrosis factor-alpha and apoptosis signal-regulating kinase 1 control reactive oxygen species release, mitochondrial autophagy, and c-Jun N-terminal kinase/p38 phosphorylation during necrotizing enterocolitis. *Oxid Med Cell Longev* 2(5):297–306, 2009.
27. Plomp PJ, Gordon PB, Meijer AJ, Hoyvik H, Seglen PO: Energy dependence of different steps in the autophagic-lysosomal pathway. *J Biol Chem* 264(12): 6699–6704, 1989.
28. Hadjiminas DJ, McMasters KM, Peyton JC, Cheadle WG: Tissue tumor necrosis factor mRNA expression following cecal ligation and puncture or intraperitoneal injection of endotoxin. *J Surg Res* 56(6):549–555, 1994.
29. Chen J, Raj N, Kim P, Andrejko KM, Deutschman CS: Intrahepatic nuclear factor-kappa B activity and alpha 1-acid glycoprotein transcription do not predict outcome after cecal ligation and puncture in the rat. *Crit Care Med* 29(3):589–596, 2001.
30. Djavaheri-Mergny M, Amelotti M, Mathieu J, Besancon F, Bauvy C, Souquere S, Pierron G, Codogno P: NF-kappaB activation represses tumor necrosis factor-alpha–induced autophagy. *J Biol Chem* 281(41):30373–30382, 2006.
31. Liu HY, Han J, Cao SY, Hong T, Zhuo D, Shi J, Liu Z, Cao W: Hepatic autophagy is suppressed in the presence of insulin resistance and hyperinsulinemia: inhibition of FoxO1-dependent expression of key autophagy genes by insulin. *J Biol Chem* 284(45):31484–31492, 2009.
32. Yelich MR: Glucoregulatory, hormonal, and metabolic responses to endotoxicosis or cecal ligation and puncture sepsis in the rat: a direct comparison. *Circ Shock* 31(3):351–363, 1990.
33. Clemens MG, Chaudry IH, Daigneau N, Baue AE: Insulin resistance and depressed gluconeogenic capability during early hyperglycemic sepsis. *J Trauma* 24(8):701–708, 1984.

Copyright © 2011 by the Shock Society. Unauthorized reproduction of this article is prohibited.